Supporting information

Surface modification of garnet fillers with polymeric sacrificial agent enables compatible interfaces of composite solid-state electrolytes

Bin Luo [a], Jintian Wu [a, c], Ming Zhang [a], Zhihao Zhang [a], Xingwei Zhang [a], Zixuan Fang [a, *], Ziqiang Xu [a, b, *], Mengqiang Wu [a, b, *]

[a]*School of Materials and Energy, University of Electronic Science and Technology of China, Chengdu 611731, Sichuan, China*

[b]*Yangtze Delta Region Institute (HuZhou), University of Electronic Science and Technology of China, Huzhou 313001, Zhejiang, China*

[c]*School of Chemical Engineering, Sichuan University of Science & Engineering, Zigong 643000, China*

Corresponding author.

* Zixuan Fang: zixuanfang@uestc.edu.cn

* Ziqiang Xu: nanterxu@uestc.edu.cn

* Mengqiang Wu: mwu@uestc.edu.cn

1. Materials and methods

1.1. Materials

N, N-dimethylformamide (DMF) was bought from Sinopharm Chemical Reagent Co. P(VDF-CTFE) (VDF: CTFE=88: 12, molar ratio) was purchased from Beijing Apsilon Technology Co. PVDF (Mw=1000000) and Lithium bis(fluorosulfonyl)imide (LiFSI, 99.5%) were obtained from Suzhou Duoduo Technology Co. Polyacrylic acid (PAA) (Mw=450,000) was purchased from Aladdin. P(VDF-CTFE), PVDF and PAA were dried in the oven for 12 hours at 80 °C prior to each use.

$Li_{6.4}La_3Zr_{1.4}Ta_{0.6}O_{12}$ (LLZTO) was synthesized using the conventional solid-phase reaction method. Stoichiometric amounts of LiOH (99.9%), La_2O_3 (99.99%), ZrO_2 (99.99%), and Ta_2O_5 (99.99%) were ball milled for 10 hours to ensure thorough mixing. The mixture was pre-calcined for 3 hours at 950 °C, with an additional 15% (by mass) of LiOH added to prevent lithium loss at high temperatures. Subsequently, the obtained powders were subjected to ball milling for 4 hours, followed by drying and sieving to obtain fine powders. The fine powders were sintered at 5°C/min, reaching a temperature of 1200 °C, and held for 3 hours. Lastly, the sintered agglomerates were ground and ball milled for 4 hours, dried and sieved to obtain LLZTO particles, and stored in a glove box.

1.2. Preparation of SSEs membranes and filler

The ceramic particles modified with PAA were labelled as LLZTO-PAA fillers, which is prepared by adding PAA and LLZTO into DMF and stirring overnight.

The SSEs membranes were prepared using the conventional solution casting method. Firstly, PAA, LLZTO and LiFSI were added to the DMF, stirring overnight to prepare the precursor solution. Subsequently, P(VDF-CTFE) was introduced into the precursor solution (20% mass concentration of all additions), and the mixture was stirred for 10 hours. The resulting slurry was coated onto the Teflon plate, after which it was dried in the vacuum drying oven for 12 hours at 40 °C, followed by an additional 30 hours at 60 °C. Finally, the dried

material was cut into electrolyte membranes with a 19 mm diameter, designated as P(VDF-CTFE)@LLZTO-PAA CSE. P(VDF-CTFE)@LLZTO CSE is an electrolyte membrane without PAA addition, and its stirring time is only 60 minutes to prevent its complete gelation. P(VDF-CTFE) SPE/P(VDF-CTFE)@PAA SPE refers to electrolyte membranes without LLZTO-PAA filler/LLZTO respectively. The fabricated electrolyte membranes were stored in the glove box for subsequent usage.

1.3. Materials characterization

The core-shell structure of the LLZTO-PAA filler was examined through transmission electron microscopy (TEM). The surface and internal microstructures of the SSEs membranes were observed using scanning electron micrographs (SEM) and energy dispersive spectrometer (EDS). X-ray diffraction (XRD) was used to analyze materials' crystal structure and composition in the 2θ range of 10° to 90° with 5°/min steps. Fourier transform infrared (FTIR) spectra was employed to analyze the reactions within the material by using the Thermo Scientific Nicolet iS50 in the 4000-400 wave number range. Raman spectra were tested on the HORIBA HR Evolution using a 532nm laser to explore information on chemical bond transitions. Thermogravimetric analysis (TGA) was conducted using the Rigaku TG-DTA8122 at 10°C/min from 30 to 600 °C. The stress-strain curves of SSEs membranes with a size of 20 mm × 40 mm × 0.1 mm were tested on INSTRON 5982 to obtain its mechanical strength. Differential scanning calorimetry (DSC) analysis was carried out on a TA DSC250 at 10°C/min ranging from 25 to 200°C. X-ray photoelectron spectroscopy (XPS) was conducted using the Thermo Scientific K-Alpha with Al Kα rays (hv=1486.6eV) and an applied voltage of 12 kV to obtain the composition at the interface.

1.4. Electrochemical performance and Membrane properties

The ionic conductivity (σ) of various SSEs was measured on the electrochemical workstation (CHI660) by stainless steel (SS) symmetric cells by electrochemical impedance spectroscopy (EIS) method at the range of 10^6- 10^{-1} Hz. σ is calculated from the EIS results and

the following equation:

$$\sigma = L/RS\#(1)$$

where L refers to the thickness of the membranes. R refers to the intrinsic resistance value of the SSEs obtained from the EIS test, and S is the contact area of the SSEs with the SS. The activation energy is calculated by ionic conductivity from 30 to 60 °C using the Arrhenius equation as follows:

$$\sigma = \sigma_0 \exp\left(-E_a/RT\right)\#(2)$$

where E_a is the activation energy required for ion transport, and σ_0, σ, R, and T refer to the pre-exponential factor, Li^+ conductivity, molar gas constant, and measurement temperature, respectively. Li||SSEs||SS cells were used to measure the electrochemical window by linear scanning voltammetry (LSV) at 1 mV s^{-1} over a range of 2.0 - 6.0 V (Li/Li^+). Li||SSEs||Li symmetric cells were experimented to get the Li^+ transference number (t_{Li^+}). The symmetric cells were measured at the applied polarization voltage (ΔV) of 10 mV for 4000 s using the Chronoamperometry method.

$$t_{Li^+} = I_s(\Delta V - I_0 R_0)/I_0(\Delta V - I_s R_s)\#(3)$$

where I_0 and I_s are the initial and steady-state currents, respectively. R_0 and R_s refer to the interface resistance values before and after the polarization of the SSEs, respectively. The assembled LFP||SSEs||Li cells were tested using cyclic voltammetry (CV) at 0.1mV s^{-1} over a voltage range of 2.5~4 V (Li/Li^+).

FTIR spectrum has been widely applied to study the crystalline form of PVDF polymers. Typically, the characteristic peaks of the α and β phases of PVDF are located at 766 and 840 cm^{-1}, respectively, but considering that we prepared P(VDF-CTFE)-based SSEs, these peaks shifted to 746 and 831 cm^{-1}, respectively. The relative content of the β-phase is calculated by the following equation when the sample is assumed to have only α and β phases:[1]

$$F(\beta) = A_\beta/((K_\beta/K_\alpha)A_\alpha + A_\beta)\#(4)$$

where $F(\beta)$ refers to the β-phase content. A_α and A_β refer to the absorbances at 746 and 831 cm^{-1}, respectively. K_α and K_β are 6.1 × 10^4 and 7.7 × 10^4 cm^2/mol, respectively, representing the absorption coefficient.

The degree of crystallinity of P(VDF-CTFE)-based SSEs membranes can be calculated semi-quantitatively according to the PVDF part by the following equation:

$$\chi = \Delta H_m / \Delta H_{100\%} \#(5)$$

Considering the multiple crystalline phases of P(VDF-CTFE), the crystallinity is calculated by the following equation:[2]

$$\chi_c = \Delta H_m / (x(\Delta H_{100\%})_\alpha + y(\Delta H_{100\%})_\beta) \#(6)$$

where χ and χ_c represent crystallinity, ΔH_m is the melting enthalpy from DSC. x and y are the weight fractions of the α and β phases, respectively. $\Delta H_{100\%}$, $(\Delta H_{100\%})_\alpha$ and $(\Delta H_{100\%})_\beta$ are the melting enthalpies of the pure crystalline phase, the pure crystalline α-phase and the pure crystalline β-phase, which have values of 104.9, 93.04 and 103.4 J/g, respectively.

1.5. Electrode fabrication and battery testing

In order to make $LiFePO_4$ or $LiCoO_2$ cathodes, $LiFePO_4$ or $LiCoO_2$, Super-P, and PVDF polymer were combined at 8: 1: 1 weight ratio and added to NMP solution to prepare a mixed slurry. The slurry was processed in an automatic coating machine with a drying temperature of 120 ℃. The mass loading of $LiFePO_4$ and $LiCoO_2$ active materials were around 1.5 and 1.8 mg cm^{-2}, respectively. When assembling the CR2032-type cells in the glove box with $LiFePO_4$ or $LiCoO_2$ cathode, lithium metal anode and SSEs, 1 μL cm^{-2} of liquid electrolyte was used at the interface to improve the interface contact. The assembled cells were run through the LAND test system for charge and discharge cycle testing and rate performance testing at 25 ℃, which $LiFePO_4$||SSEs||Li and $LiCoO_2$||SSEs||Li within a range of 2.5-4.0 V and 3-4.2 V, respectively. The symmetric lithium cells were tested on the LAND test system for lithium plating/stripping cycles and critical current density.

1.6. Theoretical calculation Methods

This study employed density functional theory (DFT) via the VASP software package to perform spin-polarized calculations and determined the associated interaction energy by the projected augmented wave (PAW) method. The Kohn Sham valence electron wave function is extended in the plane wave basis set with a cutoff energy of 400 eV. The calculation approach utilized the generalized gradient approximation (GGA) and Perdew-Burke-Ernzerhof (PBE) to simulate the exchange-correlation interactions. The convergence tolerance for the force and energy were set to 0.03 eV/Å and 10^{-5} eV, respectively. To account for van der Waals forces, the DFT-D3 method in Grimme format was employed in all calculations. The atomic relaxation was allowed for all atoms in all calculations. Three-dimensional periodic boundary conditions were applied during the simulation process. The calculations were carried out using Gaussian 16w software based on DFT with the goal of calculating the LUMO, HOMO energy levels and the electrostatic potential. The geometry configuration was optimized using the B3LYP-D3 level. The basis set selected 6–31+G (d, p). The Fukui function was applied to determine the electrophilic and nucleophilic sites, calculated according to the following equations:

$$Nucleophilic:\ f_k^+ = q_N^k - q_{N+1}^k \#(7)$$

$$Electrophilic:\ f_k^- = q_{N-1}^k + q_N^k \#(8)$$

where q^k represented the atom charge of atom k. N referred to electron number in present system.

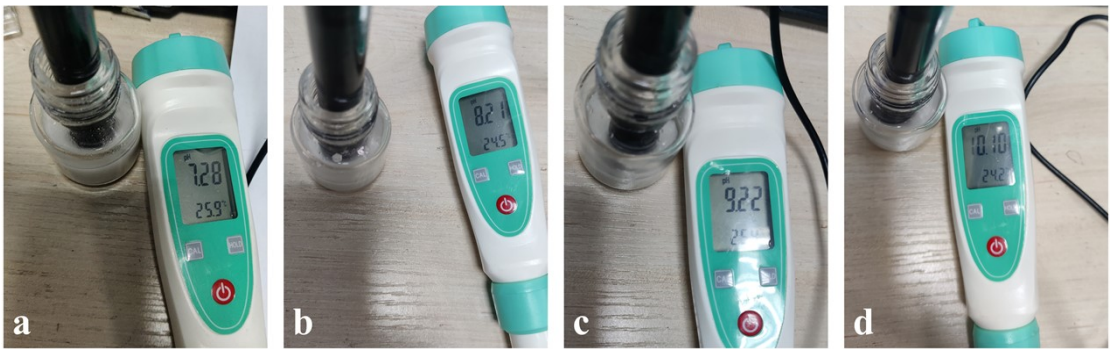

Figure S1. The pH of different LLZTO to PAA weight ratios: (a) 3:1, (b) 5:1, (c) 10:1 and (d) no PAA.

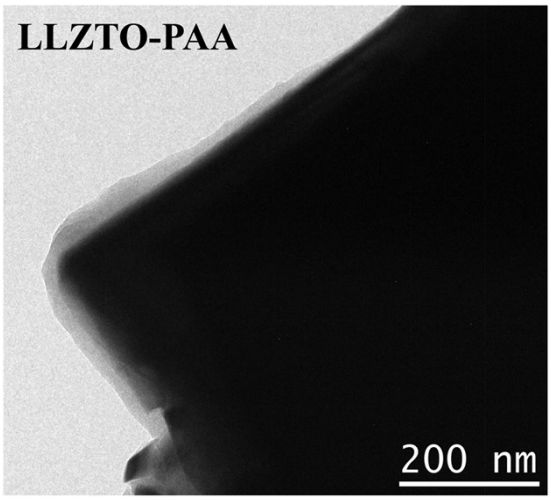

Figure S2. TEM images of LLZTO-PAA particle.

1 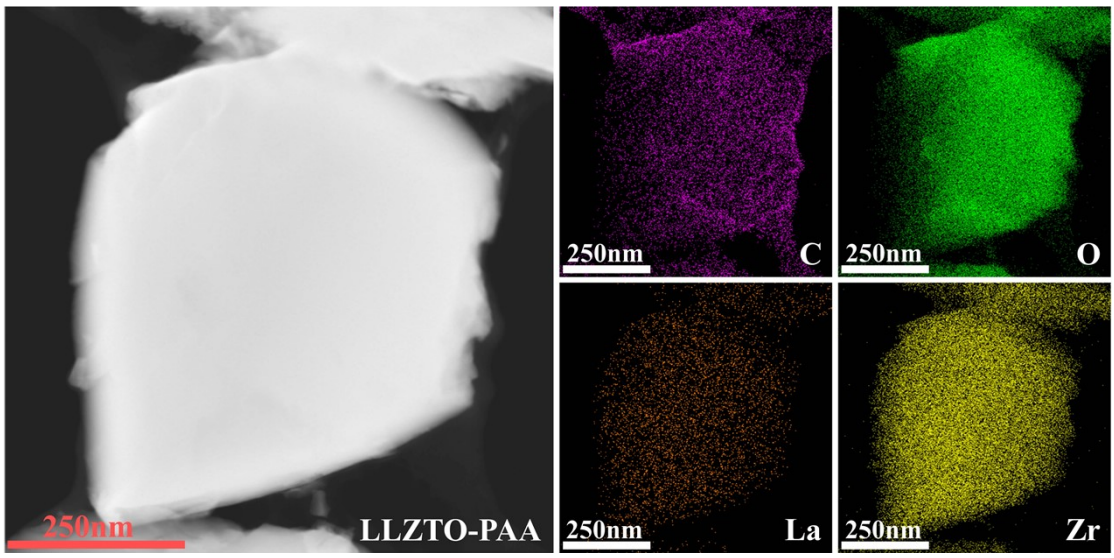

2 **Figure S3.** The corresponding EDS mapping images of the LLZTO-PAA particle.

3

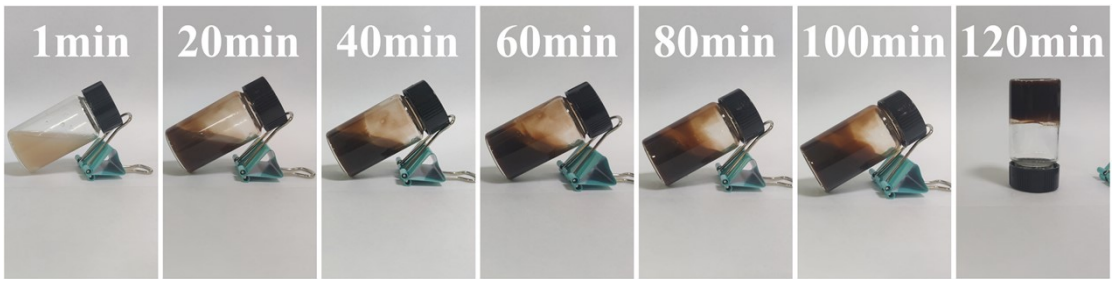

Figure S4. Optical photograph of the change in P(VDF-CTFE)@LLZTO CSE slurry fluidity at different mixing times. The resting time is 5 seconds.

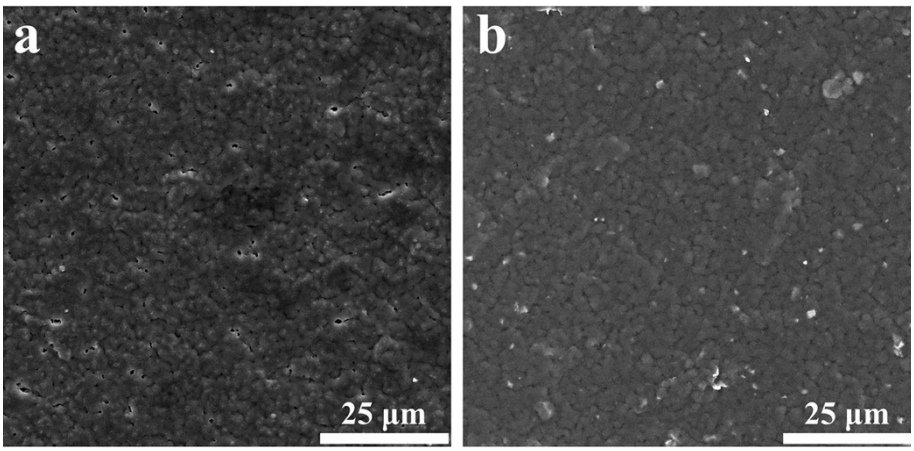

Figure S5. SEM images of the surfaces of (a) P(VDF-CTFE) SPE and (b) P(VDF-CTFE)@LLZTO-PAA CSE at low magnification.

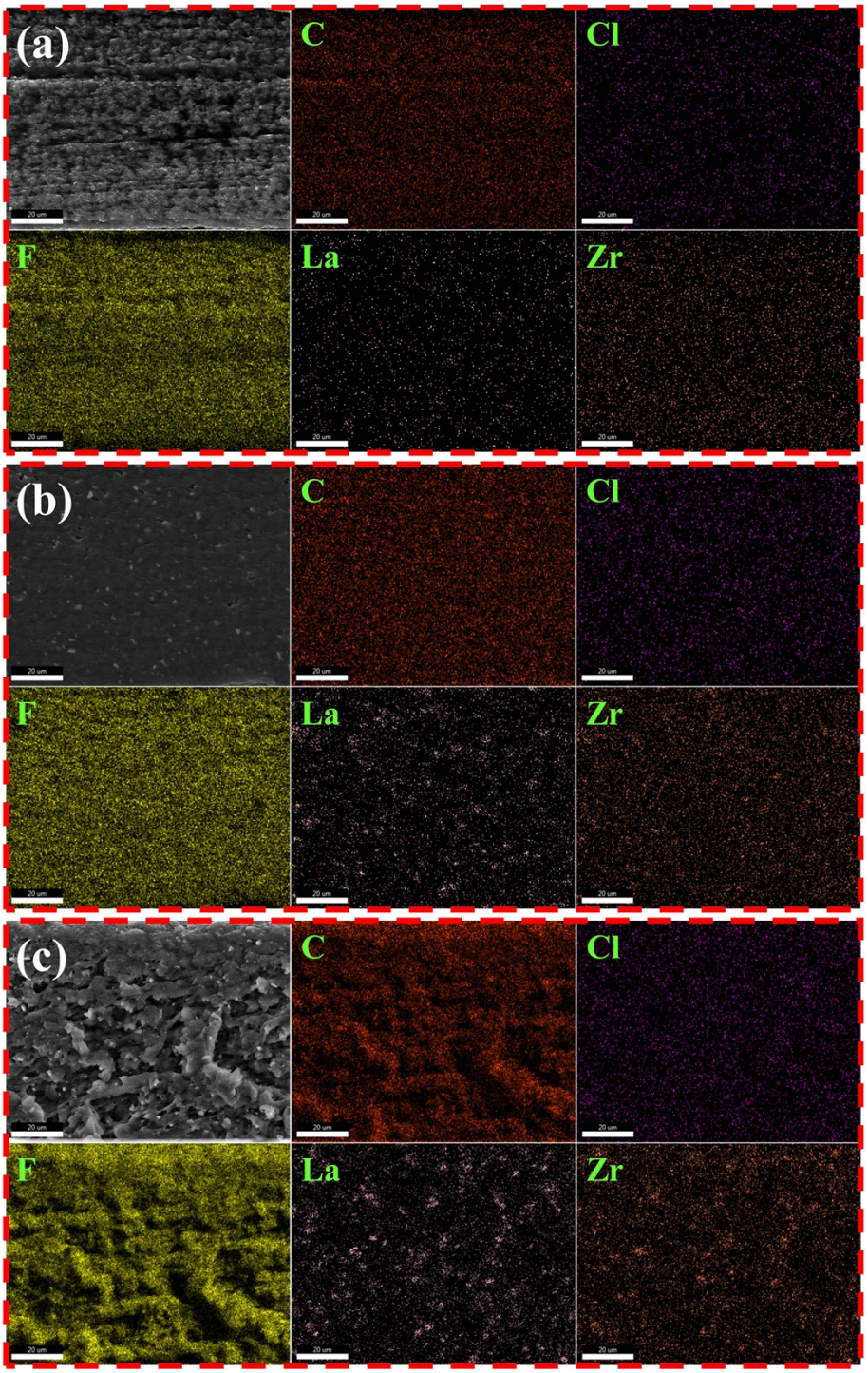

Figure S6. EDS mappings of (a) P(VDF-CTFE) SPE, (b) P(VDF-CTFE)@LLZTO-PAA CSE and (c) P(VDF-CTFE)@LLZTO CSE.

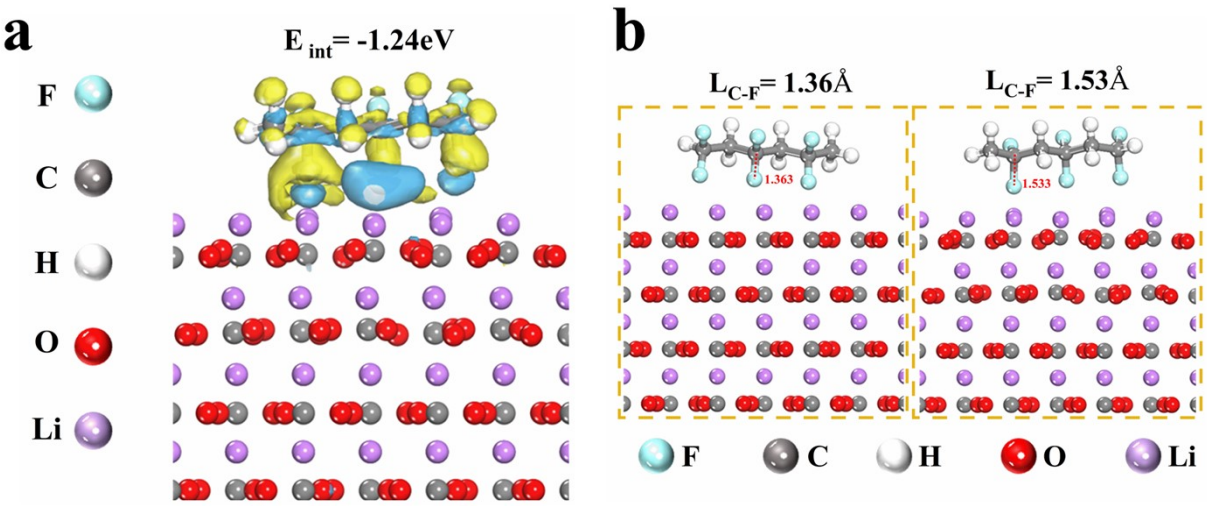

Figure S7. (a) The interaction energy of the simplified PVDF fragment with Li_2CO_3, where PVDF is the selected fragments from P(VDF-CTFE) that participates in the reaction. (b) The change in C-F bond length of PVDF before and after interacting with Li_2CO_3: before interaction (left), after interaction (right).

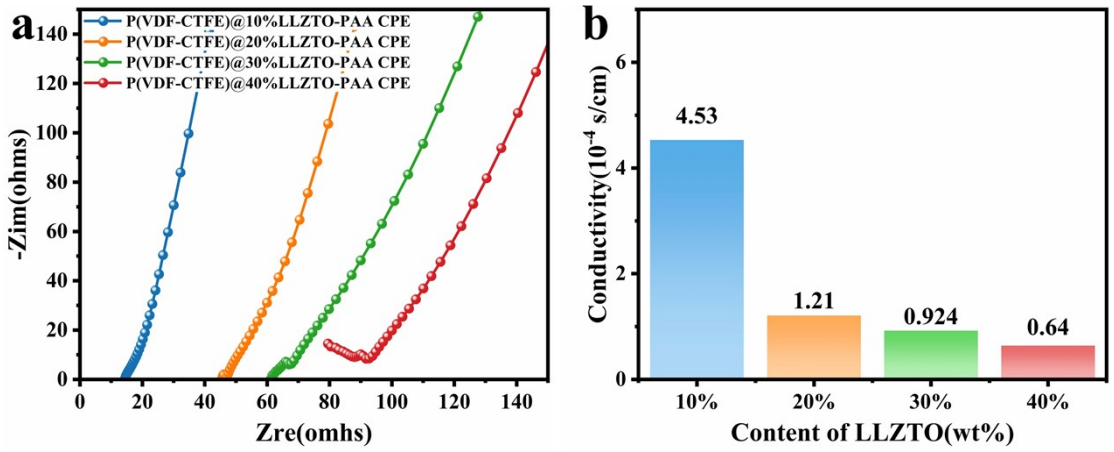

Figure S8. (a) EIS curves and (b) ionic conductivity of different P(VDF-CTFE) to LLZTO weight ratios in P(VDF-CTFE)@LLZTO-PAA CSE.

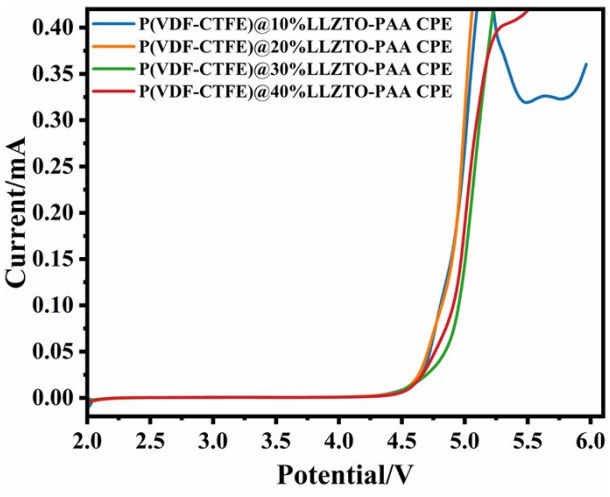

1

2 **Figure S9.** CSE LSV curves for different P(VDF-CTFE) to LLZTO weight ratios in P(VDF-

3 CTFE)@LLZTO-PAA CSE.

4

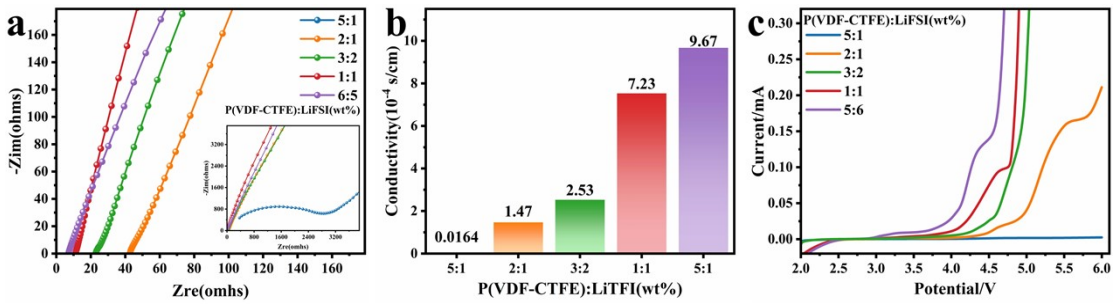

Figure S10. (a) EIS curves and (b) ionic conductivity of different P(VDF-CTFE) to LiFSI weight ratios in P(VDF-CTFE) SPE.

Suitable lithium salt addition can enhance the carrier concentration and the ionic conductivity of SSEs. Therefore, the ratio of the polymer matrix to lithium salt needs to be explored. As shown in Figure S10(a-b), the weight ratios of P(VDF-CTFE) and LiFSI are 5:1, 2:1, 3:2, 1:1 and 5:6, respectively, the corresponding ionic conductivities are 1.64×10^{-6} S cm^{-1}, 1.47×10^{-4} S cm^{-1}, 2.13×10^{-4} S cm^{-1}, 6.21×10^{-4} S cm^{-1} and 9.67×10^{-4} S cm^{-1} at room temperature. It can be observed that the ionic conductivity increases with increasing lithium salt content, indicating the excellent lithium salt dissociation ability of the high ε_r P(VDF-CTFE) copolymer matrix. However, regarding electrochemical stability, the P(VDF-CTFE) SPE membranes with high lithium salt concentration show disappointing results, with the electrochemical window test results shown in Figure S10(c). Combining ionic conductivity, electrochemical stability and cost, the most suitable weight ratio of P(VDF-CTFE) to LiFSI in the P(VDF-CTFE) SPE membrane is 3:2 and this ratio is used as the basis for the rest of the tests.

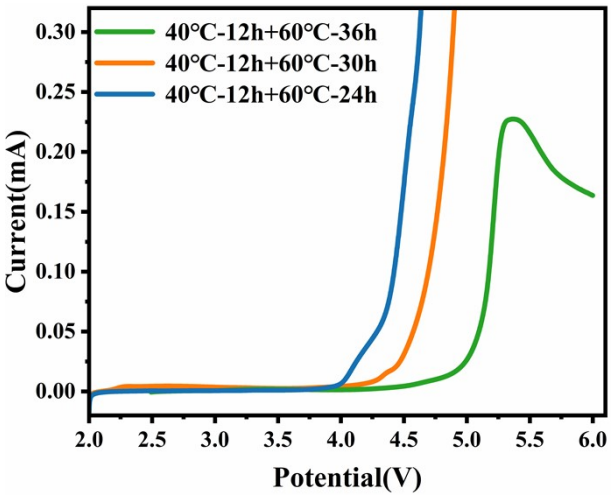

Figure S11. The P(VDF-CTFE) SPE after different drying times, 40°C-xh+60°C-yh means drying at 40°C for x hours followed at 60°C for y hours.

A series of P(VDF-CTFE) SPE samples with different residual solvent contents are prepared by adjusting the vacuum drying time, and their electrochemical windows are tested. As shown in Figure S11, it is clear that the electrochemical window of P (VDF-CTFE) SPE decreases significantly with an increasing residual solvent content.

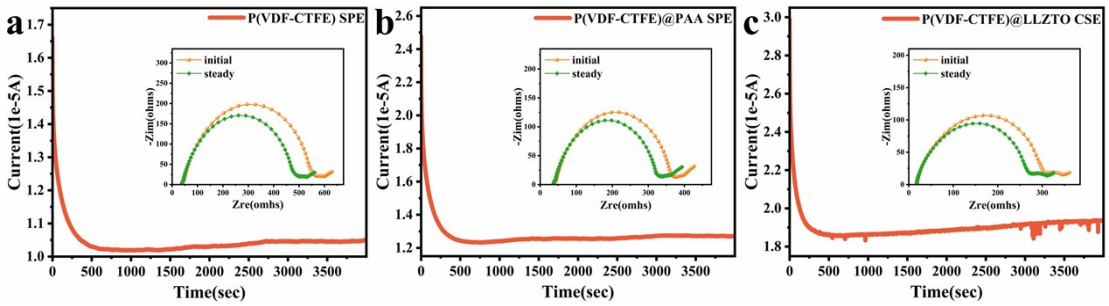

Figure S12. Chronoamperometry profile of Li/Li symmetric cell for (a) P(VDF-CTFE) SPE, (b) P(VDF-CTFE)@PAA SPE and (c) P(VDF-CTFE)@LLZTO CSE. The inset is the EIS curves before and after the polarization.

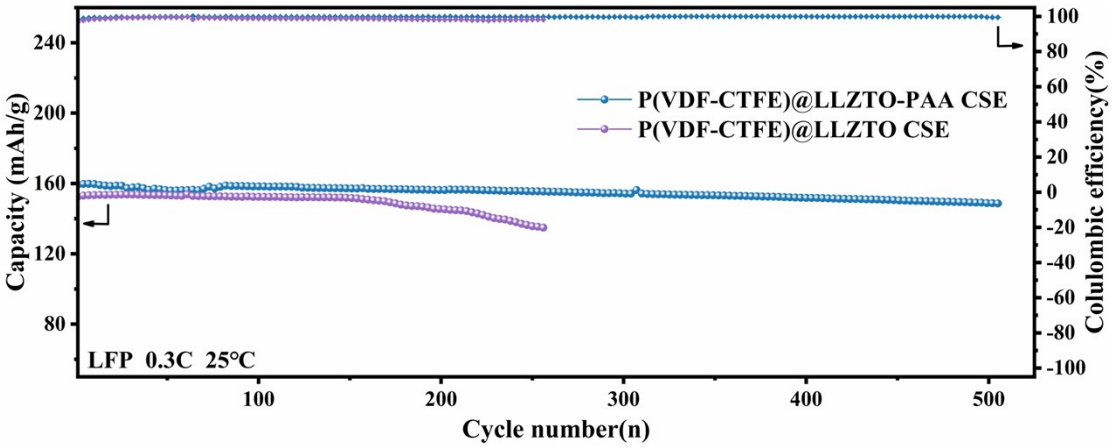

Figure S13. The long-term cycling performance at 0.3 C of LFP||SSEs||Li cells at 25°C.

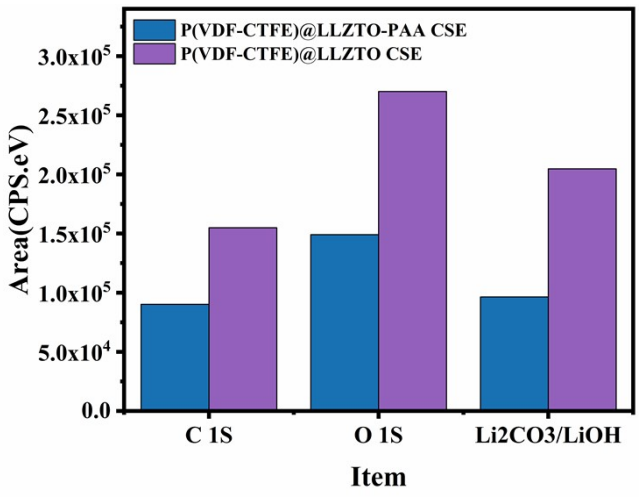

Figure S14. The areas of C 1S, O 1S and Li2CO3/LiOH in XPS spectra of lithium metal anodes from LFP||P(VDF-CTFE)@LLZTO-PAA||Li and LFP||P(VDF-CTFE)@LLZTO||Li after cycling.

Table S1. Comparison of the performance of this work with some of the reported composite solid state electrolytes.

Composite solid-state electrolyte	symmetric Li cell performance	LFP||Li cell performance	Ref.
PVDF/LiTFSI /LLZTO	0.05 mA/cm^2 1000h at 24℃	86.2 mAh/g after 200 cycles under 1C at 24℃ with capacity retention rate of 88%	3
PVDF/PEO /LiTFSI/LLZTO	0.1 mA/cm^2 1000h at 45℃	160.1 mAh/g after 200 cycles under 0.4C at 45℃ with capacity retention rate of 99%	4
PEO/LiTFSI /LLZTO/SA	0.1 mA/cm^2 900 cycles at 45℃	130.0 mAh/g after 100 cycles under 0.1C at 45℃ with capacity retention rate of 93.7%	5
PEO/LiTFSI /LLZTO/PDA	0.1mA/cm^2 800h at 25℃	134.8 mAh/g after 100 cycles under 0.1C at 25℃	6
PPC/LiTFSI /LLZTO/PDA	0.1mA/cm^2 1000h at 25℃	124 mAh/g after 100 cycles under 0.1C at 25℃ with capacity retention rate of 98.4%	7
PVDF-HPF/PEO /LiTFSI/LLZTO	0.1mA/cm^2 3000h at 60℃	161.0 mAh/g after 300 cycles under 0.2C at 60℃ with capacity retention rate of 96.1%	8
PVDF/LLZTO	0.1mA/cm^2 1050h at 25℃	149.7 mAh/g after 150 cycles under 0.1C at 25℃ with capacity retention rate of 93.6%	9
P(VDF-CTFE)/Li FSI/LLZTO/PAA	0.1mA/cm^2 3600h at 25℃	131.5 mAh/g after 650 cycles under 1C at 25℃ with capacity retention rate of 91.5%	This work

References

1. P. Martins, A. C. Lopes and S. Lanceros-Mendez, Electroactive phases of poly(vinylidene fluoride): Determination, processing and applications, *Prog. Polym. Sci.*, 2014, **39**, 683-706.

2. R. E. Sousa, M. Kundu, A. Gören, M. M. Silva, L. Liu, C. M. Costa and S. Lanceros-Mendez, Poly(vinylidene fluoride-co-chlorotrifluoroethylene) (PVDF-CTFE) lithium-ion battery separator membranes prepared by phase inversion, *RSC Adv.*, 2015, **5**, 90428-90436.

3. S. Zhang, Z. Li, Y. Guo, L. Cai, P. Manikandan, K. Zhao, Y. Li and V. G. Pol, Room-temperature, high-voltage solid-state lithium battery with composite solid polymer electrolyte with in-situ thermal safety study, *Chem. Eng. J.*, 2020, **400**, 125996.

4. C. Bai, Z. Wu, W. Xiang, G. Wang, Y. Liu, Y. Zhong, B. Chen, R. Liu, F. He and X. Guo, Poly(ethylene oxide)/Poly(vinylidene fluoride)/Li6.4La3Zr1.4Ta0.6O12 composite electrolyte with a stable interface for high performance solid state lithium metal batteries, *J. Power Sources*, 2020, **472**, 228461.

5. R.-A. Tong, L. Chen, G. Shao, H. Wang and C.-A. Wang, An integrated solvent-free modification and composite process of Li6.4La3Zr1.4Ta0.6O12/Poly(ethylene oxide) solid electrolytes: Enhanced compatibility and cycle performance, *J. Power Sources*, 2021, **492**, 229672.

6. M. Jia, Z. Bi, C. Shi, N. Zhao and X. Guo, Air-stable dopamine-treated garnet ceramic particles for high-performance composite electrolytes, *J. Power Sources*, 2021, **486**, 229363.

7. M. Jia, N. Zhao, Z. Bi, Z. Fu, F. Xu, C. Shi and X. Guo, Polydopamine-Coated Garnet Particles Homogeneously Distributed in Poly(propylene carbonate) for the Conductive and Stable Membrane Electrolytes of Solid Lithium Batteries, *ACS Appl Mater Interfaces*, 2020, **12**, 46162-46169.

8. R.-A. Tong, L. Chen, B. Fan, G. Shao, R. Liu and C.-A. Wang, Solvent-Free Process for Blended PVDF-HFP/PEO and LLZTO Composite Solid Electrolytes with Enhanced Mechanical and Electrochemical Properties for Lithium Metal Batteries, *ACS Appl. Energ. Mater.*, 2021, **4**, 11802-11812.

9. H. Liu, J. Li, W. Feng and G. Han, Strippable and flexible solid electrolyte membrane by coupling Li6.4La3Zr1.4Ta0.6O12 and insulating polyvinylidene fluoride for solid state lithium ion battery, *Ionics*, 2021, **27**, 3339-3346.